

Stabilizing non-Hermitian systems by periodic drivingJiangbin Gong (龚江滨)^{1,2} and Qing-hai Wang (王清海)¹¹*Department of Physics, National University of Singapore, 117542, Singapore*²*Centre for Computational Science and Engineering, National University of Singapore, 117542, Singapore*

(Received 29 January 2015; published 30 April 2015)

The time evolution of a system with a time-dependent non-Hermitian Hamiltonian is in general unstable with exponential growth or decay. A periodic driving field may stabilize the dynamics because the eigenphases of the associated Floquet operator may become all real. This possibility can emerge for a *continuous* range of system parameters with subtle domain boundaries. It is further shown that the issue of stability of a driven non-Hermitian Rabi model can be mapped onto the band structure problem of a class of lattice Hamiltonians. As a straightforward application, we show how to use the stability of driven non-Hermitian two-level systems (0 dimension in space) to simulate a spectrum analogous to Hofstadter's butterfly that has played a paradigmatic role in quantum Hall physics. The simulation of the band structure of non-Hermitian superlattice potentials with parity-time reversal symmetry is also briefly discussed.

DOI: [10.1103/PhysRevA.91.042135](https://doi.org/10.1103/PhysRevA.91.042135)

PACS number(s): 03.65.-w, 05.70.Ln, 11.30.Er, 42.82.Et

I. INTRODUCTION

A number of seminal results have been obtained from studies of periodically driven quantum systems [1–3]. One important example, many decades old and relevant to various research areas (such as cavity quantum electrodynamics), is the coherent Rabi oscillations induced by a driving field [4]. A recent example is the possibility of generating intriguing topological phases by periodic driving [5]. Nonperturbative periodic driving is now widely known to be useful in altering symmetry, stability, and topology of a system. The flexibility in applying a driving field also makes periodically driven systems an attractive platform to realize quantum control and quantum simulation.

Considerable theoretical activities have been devoted to time-independent non-Hermitian systems [6–12] that are relevant to optics and to quantum systems with both gain and loss. In particular, time-independent non-Hermitian systems with certain symmetries may still possess a real spectrum before reaching symmetry-breaking points. Experiments on many time-independent non-Hermitian systems were performed [13–25]. Motivated by this progress, here we explore periodically driven systems with non-Hermitian Hamiltonians. Given the vast literature about driven Hermitian systems, driven non-Hermitian systems are anticipated to be rich and enlightening as well. In the specific context of light wave propagation in waveguides, such periodic driving may be realized by a periodic modulation of the refractive index [26–28].

The dynamics of a periodically driven system is dictated by its Floquet spectrum. If the Floquet spectrum of a driven non-Hermitian system still falls on the unit circle, the Floquet operator will be unitary up to a similarity transformation. Then, upon an arbitrary number of driving periods, a Floquet eigenstate only acquires pure phase factors and a general initial state evolves via coherent phase oscillations. In this manner, periodic driving helps to stabilize the dynamics. As shown below via a non-Hermitian Rabi model, this is feasible (even when the Hamiltonian has a complex spectrum during the driving), not just for isolated points in the parameter space or for certain high-frequency driving [28], but for a *continuous*

range of system parameters using a rather general driving field. A type of coherent but norm-non-preserving oscillation, termed “generalized Rabi oscillation,” is also found.

Our computational findings are explained through a mapping between a class of driven non-Hermitian two-level systems and the band structure of a type of superlattice Hamiltonian. Depending on the explicit form of the driving, the mapped lattice Hamiltonian can be Hermitian or non-Hermitian. On the one hand, the stability of a driven non-Hermitian problem can now be connected with a conventional quantum mechanics problem, thus laying a solid starting point for studies of driven non-Hermitian systems. On the other hand, we now have a nonconventional means to simulate superlattice Hamiltonians, via a driven two-level system only. Recognizing the fundamental importance of Hofstadter's butterfly spectrum (HBS) in condensed-matter physics [29], we show how to simulate, in a straightforward manner, the HBS-like spectrum of a class of superlattice Hamiltonians. Compared with HBS realized in 2-dimensional solid-state materials [30–32], 2-dimensional ultracold gases in optical lattices [33,34], and HBS considered in 1-dimensional lattice systems [35–38], the simulation strategy proposed here is noteworthy because it is *0-dimensional* in space.

II. COMPUTATIONAL EXAMPLES

Let a non-Hermitian but time-periodic dimensionless Hamiltonian be $H(t) = H(t + T)$, where T is the driving period. Throughout we assume scaled and hence dimensionless units (with $\hbar = 1$). The initial time is $t = 0$. Unlike previous treatment for time-dependent non-Hermitian systems [39], here we stick to the normal form of the Schrödinger equation and the conventional Dirac inner product structure. The time propagator for the period of $[0, t]$ is defined as $U(t)$ and it satisfies

$$i\dot{U}(t) = H(t)U(t), \quad (1)$$

with the initial condition $U(0) = 1$. Note that the dynamics yielded by Eq. (1) with a time-dependent and non-Hermitian $H(t)$ is nonunitary in general [39]. Indeed, the normalization of a time-evolving state, initially set to be unity, may change with

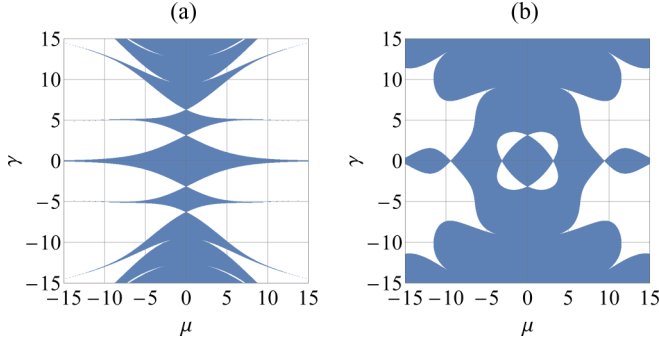


FIG. 1. (Color online) Phase diagrams for two non-Hermitian extensions of the Rabi model, with Hamiltonians $H_1(t)$ (a) defined in Eq. (5) and $H_2(t)$ (b) defined in Eq. (6). Shaded regimes represent extended unitarity and hence stabilization afforded by periodic driving. Here and in other figures, all plotted quantities are dimensionless.

time due to gain and loss in the system. The Floquet operator associated with $H(t)$ is given by $U(T)$, with its spectrum determined by the eigenvalue equation

$$U(T)|\phi_n\rangle = e^{i\beta_n}|\phi_n\rangle, \quad (2)$$

where the n th Floquet eigenstate is $|\phi_n\rangle$ with the eigenvalue $e^{i\beta_n}$. Of particular interest is the situation when all β_n are indeed real and hence $e^{i\beta_n}$ are pure phase factors. If this is true, then

$$U(T) = SDS^{-1}, \quad (3)$$

where D is a diagonal unitary matrix with phase factors $e^{i\beta_n}$ on the diagonal and S is a similarity transformation. A Floquet operator satisfying Eq. (3) is said to possess “extended unitarity.” By the Floquet theorem, after N driving periods,

$$U(NT) = U^N(T) = SD^N S^{-1}. \quad (4)$$

Thus, if extended unitarity emerges, then only pure phase factors $e^{iN\beta_n}$ enter into the time evolution operator for (arbitrary) N periods. The dynamics is hence stable over an arbitrary number of driving periods because there is no exponential growth or decay with N .

To make a driven non-Hermitian system as simple as possible, one may introduce non-Hermitian terms to a two-level Rabi model, which is very relevant to understanding the evolution of two optical polarizations in a nontransparent medium [9]. We discuss two specific examples, characterized by two real parameters γ and μ with $T = 1$. In the first example, we choose

$$H_1(t) = \gamma\sigma_z + i\mu[\cos(2\pi t) + \sin(4\pi t)]\sigma_x, \quad (5)$$

where σ_x and σ_z are Pauli matrices. The driving term $H_1(t)$ is anti-Hermitian, with two driving frequencies 2π and 4π (indicating a rather arbitrary driving). Figure 1(a) depicts the findings, with the shaded regimes representing the domains of extended unitarity. Contrary to a naive intuition, the emergence of extended unitarity is not accidental, but for a wide and continuous range of γ and μ , with highly intricate domain boundaries. It should also be stressed that the domain of extended unitarity is *not at all* the domain for $H_1(t)$ to have a real instantaneous spectrum.

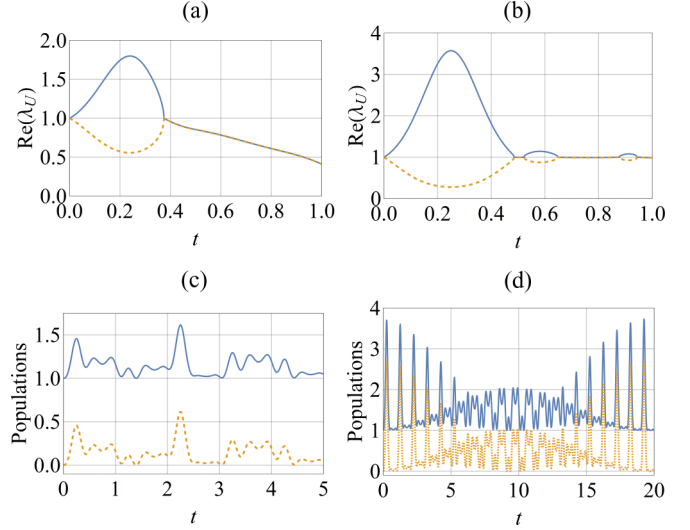


FIG. 2. (Color online) Top panels depict the real part of the eigenvalues of $U(t)$, denoted λ_U , during one period of driving. Bottom panels show generalized Rabi oscillations via populations of spin up (blue lines) and spin down (orange dashed lines). The initial state is up and the Hamiltonian is $H_1(t)$ defined in Eq. (5). In (a) and (c) $\gamma = 1$ and $\mu = 2$; in (b) and (d) $\gamma = 0.1$ and $\mu = 4$.

Let us turn to the second example with the Hamiltonian

$$H_2(t) = \gamma\sigma_z + i\mu[\sin(2\pi t) + i]\sigma_x. \quad (6)$$

The static component of H_2 now has a component parallel to the non-Hermitian driving term. Extended unitarity also emerges, with the phase diagram in Fig. 1(b) displaying again subtle boundaries. Note that the instantaneous eigenvalues of $H_2(t)$ are not real except $t/T = 0, 1/2, 1$. That is, stabilization is possible, even when the instantaneous spectrum of $H_2(t)$ is complex during almost the entire period of driving. One may introduce and then scan over more system parameters other than (μ, γ) or scan (μ, γ) in the complex domain. However, it would be challenging to present a high-dimensional phase diagram. Qualitatively similar stabilization is also observed in many other non-Hermitian variants of the Rabi model.

Next we take two sets of (μ, γ) from the domain of extended unitarity of H_1 to further digest the dynamics. First, we analyze in Fig. 2 the real part of the spectrum of $U(t)$ for $t \in [0, T]$. Because H_1 is traceless, it can be shown that if and only if the two eigenvalues of $U(t)$ have the same real parts, then the eigenvalues of $U(t)$ can be written as $\exp(\pm i\beta)$ with a real β [40]. The top two panels of Fig. 2 depict the splitting of one common real part of the eigenvalues into two, followed by a recombination of two into one. Such splitting and recombination behavior may occur several times within one period. This vividly shows that, at times not equal to multiple periods of T , $U(t)$ does not necessarily have real eigenphases. Thus, yielding extended unitarity (at $t = NT$) still allows for rather complicated and potentially exotic dynamics within one driving period. Second, let us examine the population dynamics in the presence of extended unitarity. The initial state is assumed to be the “up” state and the corresponding results are shown in the bottom panels of Fig. 2. Stable and coherent population oscillations are observed in Fig. 2(c) and

Fig. 2(d), representing a type of generalized Rabi oscillation. Interestingly, the total population on the two states may go beyond unity, which reminds us that the system dynamics is stable but not unitary. A careful check further shows that in the two shown examples the population difference (rather than the population sum) is unity at all times. This is because the driving field happens to be perpendicular to the static field, whose direction is also the direction of population measurement.

III. MAPPING STABILITY TO BAND STRUCTURE PROBLEMS

To gain insights into why stability can be thus restored, we now consider a class of traceless and non-Hermitian two-level Hamiltonians subject to one-parameter periodic modulation:

$$H(t) = [a\mathbf{n}_3 + ib(t)\mathbf{n}_1] \cdot \boldsymbol{\sigma}, \quad (7)$$

where a is time-independent and $b(t) = b(t + T)$ is a complex periodic function of t , $\boldsymbol{\sigma} = (\sigma_x, \sigma_y, \sigma_z)$, and $\{\mathbf{n}_1, \mathbf{n}_2, \mathbf{n}_3\}$ is an arbitrary but fixed set of vectors forming a right-handed basis set. For reasons to be elaborated below, a^2 is assumed to be real. We next expand $U(t)$ in the same representation, yielding

$$U(t) = u_0(t) + \sum_{i=1}^3 u_i(t)\mathbf{n}_i \cdot \boldsymbol{\sigma}, \quad (8)$$

with complex expansion coefficients $u_i(t)$ under the initial conditions $u_0(0) = 1$, and $u_i(0) = 0$ for $i = 1, 2, 3$. The two eigenvalues of $U(T)$ are hence given by $e^{\pm i\beta} = u_0(T) \pm i\sqrt{1 - u_0^2(T)}$. Clearly then, for β to be a real phase (hence extended unitarity), it is sufficient and necessary for $u_0(T)$ to be real, with $-1 \leq u_0(T) \leq 1$, such that $\beta = \arccos[u_0(T)]$. Because the eigenvalues of $U(NT)$ are simply $e^{\pm iN\beta}$, this condition also leads to $u_0(NT) = \cos(N\beta)$ and hence $-1 \leq u_0(NT) \leq 1$ for arbitrary N .

With the expansion in Eq. (8), the Schrödinger equation in Eq. (1) yields

$$\begin{aligned} \dot{u}_0(t) &= b(t)u_1(t) - iau_3(t), \\ \dot{u}_1(t) &= b(t)u_0(t) - au_2(t), \\ \dot{u}_2(t) &= au_1(t) - ib(t)u_3(t), \\ \dot{u}_3(t) &= -iau_0(t) + ib(t)u_2(t). \end{aligned} \quad (9)$$

Differentiating Eq. (9) again and canceling the first-order derivatives, we obtain the equations satisfied by $u_0(t)$ and $u_i(t)$,

$$\begin{aligned} &\left[-\frac{d^2}{dt^2} + \begin{pmatrix} b^2(t) & \dot{b}(t) & 0 & 0 \\ \dot{b}(t) & b^2(t) & 0 & 0 \\ 0 & 0 & b^2(t) & -i\dot{b}(t) \\ 0 & 0 & i\dot{b}(t) & b^2(t) \end{pmatrix} \right] \begin{pmatrix} u_0(t) \\ u_1(t) \\ u_2(t) \\ u_3(t) \end{pmatrix} \\ &= a^2 \begin{pmatrix} u_0(t) \\ u_1(t) \\ u_2(t) \\ u_3(t) \end{pmatrix}. \end{aligned} \quad (10)$$

Now we map the time variable t to a space variable x and assemble u_i as components of a wave function,

$$\Psi(x) \equiv \mathcal{N} \begin{pmatrix} u_0(x) \\ u_1(x) \end{pmatrix}, \quad \Phi(x) \equiv \mathcal{N} \begin{pmatrix} u_2(x) \\ u_3(x) \end{pmatrix}, \quad (11)$$

where \mathcal{N} is an arbitrary constant. Then Eq. (10) is seen to be the eigenvalue equation associated with a band structure problem. The mapped band structure problem is naturally decoupled to two with identical spectra,

$$\left[-\frac{d^2}{dx^2} + b^2(x) + \frac{db(x)}{dx}\sigma_x \right] \Psi(x) = a^2\Psi(x), \quad (12)$$

$$\left[-\frac{d^2}{dx^2} + b^2(x) + \frac{db(x)}{dx}\sigma_y \right] \Phi(x) = a^2\Phi(x). \quad (13)$$

Equations (12) and (13) can be further simplified by defining

$$\psi^\pm(x) \equiv \mathcal{N} [u_0(x) \pm u_1(x)], \quad (14)$$

$$\phi^\pm(x) \equiv \mathcal{N} [u_2(x) \mp iu_3(x)]. \quad (15)$$

The one-dimensional wave functions $\psi^\pm(x)$ and $\phi^\pm(x)$ thus defined satisfy the following identical Schrödinger equations,

$$\left[-\frac{d^2}{dx^2} + V^\pm(x) \right] \psi^\pm(x) = a^2\psi^\pm(x), \quad (16)$$

$$\left[-\frac{d^2}{dx^2} + V^\pm(x) \right] \phi^\pm(x) = a^2\phi^\pm(x), \quad (17)$$

which describe a particle of mass 1/2 moving in one of the two periodic potentials

$$V^\pm(x) \equiv b^2(x) \pm \frac{db(x)}{dx} \quad (18)$$

of lattice constant T ; i.e., $V^\pm(x + T) = V^\pm(x)$. For example, if $b(t)$ is a time-periodic square function, then $V^\pm(x)$ will become a generalized Dirac-Kronig-Penney model as it comprises δ potentials with alternating signs. Interestingly, because $V^+(x)$ and $V^-(x)$ naturally form a supersymmetric potential pair, they yield identical spectrum [41]. As such, nontrivial solutions to Eq. (16) [or Eq. (17)] with a common eigenvalue a^2 should exist for both $\psi^+(x)$ and $\psi^-(x)$ [or $\phi^+(x)$ and $\phi^-(x)$]. For simplicity, we may use ψ to represent one of ψ^\pm or ϕ^\pm , and V for the corresponding V^\pm . Due to this mapping, below we do not clearly distinguish between t and x variables when the context is clear.

According to the Floquet theorem, the Bloch wave function $\psi(x)$ satisfies the twisted boundary conditions, i.e.,

$$\psi(x) = e^{ikx}\tilde{\psi}_k(x), \quad (19)$$

where k is called the quasimomentum when it is real, and $\tilde{\psi}_k(x)$ is a periodic function of x , of the same period T as the mapped Hamiltonian in Eqs. (16) or (17).

The extended unitarity condition $-1 \leq u_0(NT) \leq 1$ can now be better digested. Intuitively, if there is a complex eigenphase β , then the condition $-1 \leq u_0(NT) \leq 1$ is violated because of an exponential growth of $u_0(NT)$ vs N . But if this exponential growth occurs, then $\psi^\pm(NT) = \mathcal{N}[u_0(NT) \pm u_1(NT)]$ diverges with N and hence cannot be a Bloch eigenfunction at energy a^2 within a continuous energy band [see Eq. (16)]. That is to say, in order to achieve stabilization via periodic driving, the system parameters must be chosen such that the driving field profile $b(t)$ generates a mapped potential $V(x)$ that admits Bloch band wave functions at energy eigenvalue a^2 . On the other hand, if $\psi(x)$ is a Bloch

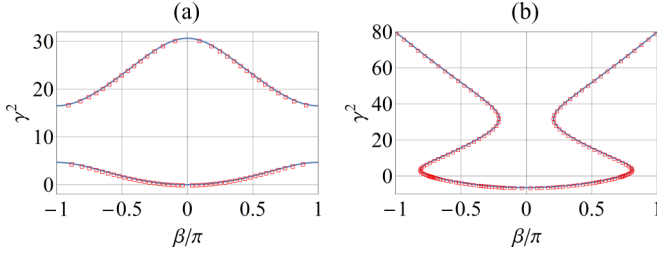


FIG. 3. (Color online) Identical dispersion relations obtained by direct band-structure calculations using V_1^+ or V_2^+ defined in Eqs. (20) and (21) (blue lines) or by checking whether extended unitarity occurs (red squares). Panel (a) is for H_1 with $\mu = 2$ and panel (b) is for H_2 with $\mu = 4$. The negative γ^2 part in (b) is obtained by scanning the parameter γ in the purely imaginary domain. Results here confirm our theoretical mapping.

band wave function, then one can indeed construct from $\psi(x)$ a solution of $u_0(t)$ satisfying $-1 \leq u_0(NT) \leq 1$ and its initial condition (see Appendix B for details). We have thus identified a mapping between the band structure of $V(x)$ and the stability in a driven non-Hermitian system. More detailed analysis shows that through this general mapping, the real eigenphase β of $U(T)$ becomes the Bloch quasimomentum times the lattice period in the band structure problem for $\psi(x)$.

Returning to the case of $H_1(t)$, $\mathbf{n}_1 = \hat{x}$, $\mathbf{n}_3 = \hat{z}$, we have $a = \gamma$, $b(t) = \mu[\cos(2\pi t) + \sin(4\pi t)]$. Then the mapped lattice potential becomes

$$V_1^\pm(x) = \mu^2[\cos^2(2\pi x) + \sin^2(4\pi x) + 2\cos(2\pi x)\sin(4\pi x)] \pm 2\pi\mu[-\sin(2\pi x) + 2\cos(4\pi x)], \quad (20)$$

a real superlattice potential. In the same manner, $H_2(t)$ is mapped to a lattice potential

$$V_2^\pm(x) = \mu^2[\sin^2(2\pi x) - 1 + 2i\sin(2\pi x)] \pm 2\pi\mu\cos(2\pi x). \quad (21)$$

The potential $V_2(x)$ is seen to be complex, but it is invariant upon a joint time reversal and parity (\mathcal{PT}) operation, the so-called \mathcal{PT} invariance. The possibility of having a real spectrum (a^2 is constructed to be real) under \mathcal{PT} symmetry ensures that we still possibly have Bloch wave functions for $V_2(x)$. Therefore, for both examples of $H_1(t)$ and $H_2(t)$, the phase diagrams in Fig. 1 can now be understood as the collection of all possible real band energy eigenvalues $a^2 = \gamma^2$ as a function of a second system parameter μ . The origin of the boundaries seen in Fig. 1 is hence identified as the presence of energy gaps for the real potential $V_1(x)$ or the \mathcal{PT} -symmetric complex potential $V_2(x)$. To further check our understandings, for one value of μ we record β when extended unitarity occurs and then plot γ^2 vs β for H_1 and H_2 (red squares). The results are then compared in Fig. 3 with band dispersion relations obtained from direct band-structure calculations for V_1^+ or V_2^+ . The agreement seen in Fig. 3 confirms our exact mapping described above.

IV. QUANTUM SIMULATION

To motivate potential experimental interest, let us now investigate two non-Hermitian Rabi models upon introducing

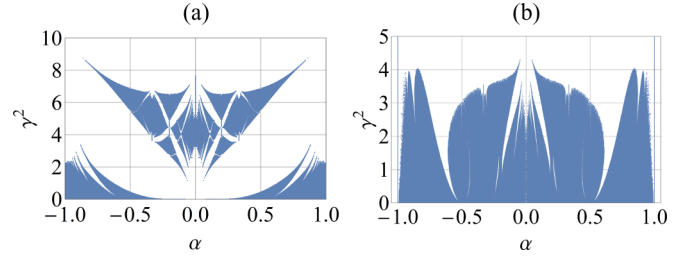


FIG. 4. (Color online) Simulation of a phase pattern analogous to Hofstadter's butterfly spectrum (HBS) (a) and an extension of HBS for non-Hermitian but \mathcal{PT} -symmetric Hamiltonians (b), using driven non-Hermitian Hamiltonians $H_3(t)$ (a) and $H_4(t)$ (b) defined in Eqs. (22) and (23) with both $\mu = 2$. Blue dots represent extended unitarity restored by periodic driving.

a parameter α that describes the period ratio of two commensurable driving periods. Consider first

$$H_3(t) = \gamma\sigma_z + i\mu[\cos(2\pi t) + \cos(2\alpha\pi t)]\sigma_x. \quad (22)$$

If the parameter α is a rational number with $\alpha = p/q$ (p, q two co-prime integers), the mapped superlattice potential V_3^\pm , comprising a base lattice of period unity and additional superlattice components, still has a period q . The α parameter hence resembles the role of the magnetic flux per plaquette in the HBS Hamiltonian of the original quantum Hall problem [29]. For a fixed value of μ , we obtain the phase diagram of extended unitarity in terms of γ^2 vs a varying rational α . The results are shown in Fig. 4(a). The shown phase diagram of extended unitarity is indeed highly similar to HBS. In particular, many clear gaps and intriguing domain boundary profiles are found. This is achieved without the use of a magnetic field, a clean 2-dimensional material, or even a 1-dimensional lattice potential. Given the paradigmatic role of HBS in understanding quantum Hall physics [29], our findings in Fig. 4(a) have paved a nonconventional way towards the simulation of quantum Hall physics, including topological phase transitions. For example, it will be valuable to examine the topological characterizations and implications of the gaps seen in Fig. 4(a).

Next we consider

$$H_4(t) = \gamma\sigma_z + i\mu[\sin(2\pi t) + i\cos(2\alpha\pi t)]\sigma_x. \quad (23)$$

In this case, the associated superlattice potential $V_4(x)$ is non-Hermitian but is apparently \mathcal{PT} -symmetric. This situation hence represents a complex extension of the original HBS problem. Interestingly, the resulting phase diagram of H_4 shown in Fig. 4(b) has many fewer gaps and is thus quite different from a conventional HBS. Upon a careful inspection, the lack of many gaps here is found to be connected with \mathcal{PT} -symmetry breaking in the mapped problem. That is, a gap often closes at the critical quasimomentum value for which the spectrum of a \mathcal{PT} -symmetric lattice becomes complex [see Fig. 3(b)].

V. CONCLUSIONS

Stabilization of a non-Hermitian system by periodic driving is feasible in general and thus does not need the instantaneous spectrum of the Hamiltonian to be real. This extends

opportunities in studies of non-Hermitian systems. Stabilization can be also achieved in other non-Hermitian systems with more levels. Extended unitarity found here is useful for quantum simulation. We also note a recent stimulating study [42], where the emphasis is placed on how \mathcal{PT} symmetry of driven systems is broken by a close-to-resonance perturbation. The mapping established here can be used to explain some results in Ref. [42].

ACKNOWLEDGMENT

Q.-h.W. would like to thank Prof. Weixiao Shen for enlightening comments regarding the highly complex nature of periodically driven dynamical systems.

APPENDIX A: QUASIMOMENTUM

In this Appendix, we show that regardless of the explicit form of the periodic potential $V(x)$, if there exists a Bloch wave function $e^{ikx}\tilde{\psi}_k(x)$ with quasimomentum k and the energy eigenvalue a^2 , there must exist another Bloch wave function $e^{-ikx}\tilde{\psi}_{-k}(x)$ with quasimomentum $-k$ and the same energy eigenvalue. To see this clearly, let us consider Eq. (16) in the Fourier space of $\tilde{\psi}_k(x)$, namely,

$$\left(k + \frac{2\pi m}{T}\right)^2 C_{k,m} + \sum_n V_{mn} C_{k,n} = a^2 C_{k,m}, \quad (\text{A1})$$

where

$$V_{mn} \equiv \frac{T}{2\pi} \int_0^{\frac{2\pi}{T}} \exp\left[i\frac{2\pi(n-m)x}{T}\right] V(x) dx \quad (\text{A2})$$

and $C_{k,m}$ are the Fourier expansion coefficients of the periodic function $\tilde{\psi}_k(x)$. Consider now a matrix transpose of the matrix $V_{mn} - (k + \frac{2\pi m}{T})^2 \delta_{mn}$. Because the matrix transpose has the same eigenvalues, we have

$$\left(k + \frac{2\pi m}{T}\right)^2 D_{k,m} + \sum_n [V_{mn}]^\top D_{k,n} = a^2 D_{k,m}, \quad (\text{A3})$$

where $D_{k,m}$ is the eigenvector of the transpose matrix. By definition of V_{mn} in Eq. (A2), we have

$$[V_{mn}]^\top = V_{-m,-n}. \quad (\text{A4})$$

Thus, Eq. (A3) becomes

$$\left(k + \frac{2\pi m}{T}\right)^2 D_{k,m} + \sum_n V_{-m,-n} D_{k,n} = a^2 D_{k,m}. \quad (\text{A5})$$

Let $m \rightarrow -m$, $n \rightarrow -n$, and define $\bar{D}_{-k,m} \equiv D_{k,-m}$; one now has

$$\left(-k + \frac{2\pi m}{T}\right)^2 \bar{D}_{-k,m} + \sum_n V_{mn} \bar{D}_{-k,n} = a^2 \bar{D}_{-k,m}. \quad (\text{A6})$$

Equation (A6) indicates the following: for the periodic potential $V(x)$ with Fourier components V_{mn} , there also exists an eigenvector with eigenvalue of a^2 and quasimomentum $-k$.

Note that for the special case of pure anti-Hermitian driving, $b(t)$ and hence $V^\pm(x)$ are real functions; the differential equations (16) and (17) are real. We may choose $\tilde{\psi}_{-k}(x) = [\tilde{\psi}_k(x)]^*$, where $*$ stands for complex conjugate. In general,

$\tilde{\psi}_k(x)$ and $\tilde{\psi}_{-k}(x)$ are not simply related. In any case, $e^{ikx}\tilde{\psi}_k(x)$ and $e^{-ikx}\tilde{\psi}_{-k}(x)$ are two linearly independent solutions to Eq. (16) [or Eq. (17)].

APPENDIX B: EXTENDED UNITARITY AND BLOCH BAND SOLUTIONS

Now let us discuss more the equivalence between extended unitarity defined in the main text and the existence of Bloch band wave functions. Mathematically, both $[u_0(t), u_1(t), u_2(t), u_3(t)]$ defined in the main text and the above-mentioned Bloch eigenfunctions are solutions of Eq. (3) of the main text, but with different boundary conditions. In particular, in our periodic-driving problem, the time evolution operator must satisfy the initial condition $U(0) = 1$, namely,

$$\begin{pmatrix} u_0(0) \\ u_1(0) \\ u_2(0) \\ u_3(0) \end{pmatrix} = \begin{pmatrix} 1 \\ 0 \\ 0 \\ 0 \end{pmatrix}. \quad (\text{B1})$$

However, Bloch eigenfunctions satisfy the twisted boundary conditions defined in Eq. (19) (see the main text), and they represent stable energy band solutions only when the exponent k in the twisted boundary condition is real.

For a four-component system depicted by Eq. (10), in total we have four linearly independent solutions associated with a^2 . A simple observation of Eqs. (12) and (13) indicates that for a fixed energy eigenvalue a^2 and a fixed exponent k in the twisted boundary condition, Eq. (10) can yield two solutions. Hence, for a given Hamiltonian in Eq. (1) in the main text, i.e., with a and all the parameters in $b(t)$ fixed, a general solution of the time propagator can be expressed as a linear combination of the four Bloch eigenfunctions characterized by two exponents k_1 and k_2 ,

$$\begin{pmatrix} u_0(t) \\ u_1(t) \\ u_2(t) \\ u_3(t) \end{pmatrix} = A e^{ik_1 t} \begin{pmatrix} u_0^{(1)}(t) \\ u_1^{(1)}(t) \\ u_2^{(1)}(t) \\ u_3^{(1)}(t) \end{pmatrix} + B e^{ik_2 t} \begin{pmatrix} u_0^{(2)}(t) \\ u_1^{(2)}(t) \\ u_2^{(2)}(t) \\ u_3^{(2)}(t) \end{pmatrix} \\ + C e^{ik_1 t} \begin{pmatrix} u_0^{(3)}(t) \\ u_1^{(3)}(t) \\ u_2^{(3)}(t) \\ u_3^{(3)}(t) \end{pmatrix} + D e^{ik_2 t} \begin{pmatrix} u_0^{(4)}(t) \\ u_1^{(4)}(t) \\ u_2^{(4)}(t) \\ u_3^{(4)}(t) \end{pmatrix}, \quad (\text{B2})$$

where we mapped x back to t for comparison. Now, to switch between a solution representing the time propagator and the Bloch wave functions, we only need to find a set of parameters A , B , C , and D such that the left-hand side of Eq. (B2) at $t = 0$ satisfies the initial condition defined in Eq. (B1). By Cramer's rule, this can be done so long as there is a nonvanishing Wronskian (at $t = 0$) of the four Bloch wave functions, with the Wronskian given by

$$W(t) \equiv \begin{vmatrix} u_0^{(1)}(t) & u_0^{(2)}(t) & u_0^{(3)}(t) & u_0^{(4)}(t) \\ u_1^{(1)}(t) & u_1^{(2)}(t) & u_1^{(3)}(t) & u_1^{(4)}(t) \\ u_2^{(1)}(t) & u_2^{(2)}(t) & u_2^{(3)}(t) & u_2^{(4)}(t) \\ u_3^{(1)}(t) & u_3^{(2)}(t) & u_3^{(3)}(t) & u_3^{(4)}(t) \end{vmatrix}. \quad (\text{B3})$$

Such a Wronskian can be computed from Abel's formula. Since the Hamiltonian is not singular at any time, the Wronskian never vanishes. That is, regardless of the nature of the solution $[u_0(t), u_1(t), u_2(t), u_3(t)]$, it can be always expanded by four linearly independent solutions with different exponent k (real or complex).

When both exponents k_1 and k_2 are real, that is, when the corresponding solutions are the Bloch band wave functions, then we have $k_1 = -k_2$ based on our analysis in Appendix A. The existence of such Bloch band

wave functions suffices to yield a time propagator solution $[u_0(NT), u_1(NT), u_2(NT), u_3(NT)]$ satisfying its initial condition. More importantly, in this case, $u_0(NT)$ constructed via Eq. (B2) must be stable with time and hence extended unitarity emerges. On the other hand, if there is extended unitarity and hence $u_0(NT)$ does not blow up with N , then the exponents k_1, k_2 must be real, and as such the expansion in Eq. (B2) must hold again with $k_1 = -k_2$. Furthermore, if $u_0(T) = \cos(\beta)$, then $u_0(NT) = \cos(N\beta)$. From Eq. (B2) one directly observes that the quasimomentum $k_1 = -k_2$ must be given by $\pm\beta/T$.

-
- [1] G. Casati and B. V. Chirikov, *Quantum Chaos: Between Order and Disorder* (Cambridge University Press, New York, 1995).
- [2] M. Grifoni and P. Hänggi, *Phys. Rep.* **304**, 229 (1998).
- [3] S. Kohler, J. Lehmann, and P. Hänggi, *Phys. Rep.* **406**, 379 (2005).
- [4] I. I. Rabi, *Phys. Rev.* **49**, 324 (1937); **51**, 652 (1937).
- [5] See, e.g., D. Y. H. Ho and J. B. Gong, *Phys. Rev. B* **90**, 195419 (2014).
- [6] C. M. Bender and S. Boettcher, *Phys. Rev. Lett.* **80**, 5243 (1998).
- [7] C. M. Bender, D. C. Brody, and H. F. Jones, *Phys. Rev. Lett.* **89**, 270401 (2002).
- [8] C. M. Bender, *Rep. Prog. Phys.* **70**, 947 (2007).
- [9] M. V. Berry, *J. Opt.* **13**, 115701 (2011).
- [10] S. Longhi, *Phys. Rev. Lett.* **103**, 123601 (2009).
- [11] C. T. West, T. Kottos, and T. Prosen, *Phys. Rev. Lett.* **104**, 054102 (2010).
- [12] A. Mostafazadeh, *J. Math. Phys.* **43**, 205 (2002); **43**, 2814 (2002).
- [13] Z. H. Musslimani, K. G. Makris, R. El-Ganainy, and D. N. Christodoulides, *Phys. Rev. Lett.* **100**, 030402 (2008).
- [14] K. G. Makris, R. El-Ganainy, D. N. Christodoulides, and Z. H. Musslimani, *Phys. Rev. Lett.* **100**, 103904 (2008).
- [15] A. Guo, G. J. Salamo, D. Duchesne, R. Morandotti, M. Volatier-Ravat, V. Aimez, G. A. Siviloglou, and D. N. Christodoulides, *Phys. Rev. Lett.* **103**, 093902 (2009).
- [16] C. E. Rüter, K. G. Makris, R. El-Ganainy, D. N. Christodoulides, M. Segev, and D. Kip, *Nat. Phys.* **6**, 192 (2010).
- [17] J. Schindler, A. Li, M. C. Zheng, F. M. Ellis, and T. Kottos, *Phys. Rev. A* **84**, 040101 (2011).
- [18] A. Regensburger, C. Bersch, M. A. Miri, G. Onishchukov, D. N. Christodoulides, and U. Peschel, *Nature (London)* **488**, 167 (2012).
- [19] A. Regensburger, M. A. Miri, C. Bersch, J. Näger, G. Onishchukov, D. N. Christodoulides, and U. Peschel, *Phys. Rev. Lett.* **110**, 223902 (2013).
- [20] M. Brandstetter, M. Liertzer, C. Deutsch, P. Klang, J. Schöberl, H. E. Türeci, G. Strasser, K. Unterrainer, and S. Rotter, *Nat. Commun.* **5**, 4034 (2014).
- [21] B. Peng, S. K. Ozdemir, S. Rotter, H. Yilmaz, M. Liertzer, F. Monifi, C. M. Bender, F. Nori, and L. Yang, *Science* **346**, 328 (2014).
- [22] B. Peng, S. K. Ozdemir, F. Lei, F. Monifi, M. Gianfreda, G. L. Long, S. Fan, F. Nori, C. M. Bender, and L. Yang, *Nat. Phys.* **10**, 394 (2014).
- [23] H. Jing, S. K. Özdemir, X.-Y. Lü, J. Zhang, L. Yang, and F. Nori, *Phys. Rev. Lett.* **113**, 053604 (2014).
- [24] L. Feng, Z. J. Wong, R.-M. Ma, Y. Wang, and X. Zhang, *Science* **346**, 972 (2014).
- [25] M. Liertzer, L. Ge, A. Cerjan, A. D. Stone, H. E. Türeci, and S. Rotter, *Phys. Rev. Lett.* **108**, 173901 (2012).
- [26] G. Della Valle, M. Ornigotti, E. Cianci, V. Foglietti, P. Laporta, and S. Longhi, *Phys. Rev. Lett.* **98**, 263601 (2007).
- [27] A. Szameit, Y. V. Kartashov, F. Dreisow, M. Heinrich, T. Pertsch, S. Nolte, A. Tünnermann, V. A. Vysloukh, F. Lederer, and L. Torner, *Phys. Rev. Lett.* **102**, 153901 (2009).
- [28] X. Luo, J. Huang, H. Zhong, X. Qin, Q. Xie, Y. S. Kivshar, and C. Lee, *Phys. Rev. Lett.* **110**, 243902 (2013).
- [29] D. R. Hofstadter, *Phys. Rev. B* **14**, 2239 (1976).
- [30] C. R. Dean *et al.*, *Nature (London)* **497**, 598 (2013).
- [31] L. A. Ponomarenko *et al.*, *Nature (London)* **497**, 594 (2013).
- [32] B. Hunt *et al.*, *Science* **340**, 1427 (2013).
- [33] M. Aidelsburger, M. Atala, M. Lohse, J. T. Barreiro, B. Paredes, and I. Bloch, *Phys. Rev. Lett.* **111**, 185301 (2013).
- [34] H. Miyake, G. A. Siviloglou, C. J. Kennedy, W. C. Burton, and W. Ketterle, *Phys. Rev. Lett.* **111**, 185302 (2013).
- [35] J. Wang and J. B. Gong, *Phys. Rev. A* **77**, 031405 (2008).
- [36] L. J. Lang, X. Cai, and S. Chen, *Phys. Rev. Lett.* **108**, 220401 (2012).
- [37] A. Celi, P. Massignan, J. Ruseckas, N. Goldman, I. B. Spielman, G. Juzeliunas, and M. Lewenstein, *Phys. Rev. Lett.* **112**, 043001 (2014).
- [38] L. W. Zhou, H. L. Wang, D. Y. H. Ho, and J. B. Gong, *Eur. Phys. J. B* **87**, 204 (2014).
- [39] J. B. Gong and Q.-h. Wang, *Phys. Rev. A* **82**, 012103 (2010); *J. Phys. A* **46**, 485302 (2013).
- [40] $H(t)$ is traceless; Liouville's formula $i \frac{\partial}{\partial t} \text{Det}[U(t)] = \text{Tr}[H(t)] \text{Det}[U(t)]$ indicates that $\text{Det}[U(t)]$ must stay at unity. Two eigenvalues of U having the same real parts then indicate real eigenphases of U .
- [41] A supersymmetry pair is often discussed under Dirichlet boundary conditions; see, e.g., F. Cooper, A. Khare, and U. Sukhatme, *Phys. Rep.* **251**, 267 (1995). It is nevertheless found to be also true here.
- [42] Y. N. Joglekar, R. Marathe, P. Durganandini, and R. K. Pathak, *Phys. Rev. A* **90**, 040101 (2014).